



A Novel Fractional Analytical Technique for the Time-space Fractional Equations Appearing in Oil Pollution

P. Jalili^a, B. Jalili^{*a}, A. Shateri^a, D. Domiri Ganji^b

^a Department of Mechanical Engineering, North Tehran Branch, Islamic Azad University, Tehran, Iran

^b Department of Mechanical Engineering, Babol Noshirvani University of Technology, Babol, Iran

PAPER INFO

Paper history:

Received 20 August 2022

Received in revised form 13 September 2022

Accepted 18 September 2022

Keywords:

Homotopy Perturbation Method

Oil spills

Diffusion and Allen–Cahn Equations

Fractional Derivative

ABSTRACT

Oil spills in the seas and oceans cause pollution and have many destructive environmental effects. The diffusion (parabolic) equations are the most reasonable option to model the propagation of this leakage and contamination. These equations allow statistics regarding the amount of oil that has outreached the ocean outlet, to be used as initial and boundary conditions for a mathematical model of oil diffusion and alteration in seas. As it involves the hyperbolic (advection/wave) component of the equation, the most reasonable choices are diffusion and Allen–Cahn (AC) equations, which are difficult to solve numerically. Equations of diffusion and Allen–Cahn were solved with different degrees of fractional derivatives ($\alpha=0.25$, $\alpha=0.5$, $\alpha=0.75$ and $\alpha=0.75$), and the oil pollution concentration was obtained at a specific time and place. This study adopts the homotopy perturbation method (HPM) for nonlinear Allen–Cahn (AC) equation and time fractional diffusion equation to express oil pollution in the water. Fractional derivatives are portrayed in the sense of Caputo. Two presented examples illustrate the applicability and validity of the proposed method. Pollution concentrations in flow field over an interval of time and space for different degrees of fractional derivation are shown. At lower fraction derivative degrees, the pollution concentration behavior is nonlinear, and as the degree of fraction derivation increases to one, the nonlinear behavior of the pollution concentration decreases. The results produced by the suggested technique compared to the exact solutions shows that it is efficient and convenient; it is also reduces computational time.

doi: 10.5829/ije.2022.35.12c.15

1. INTRODUCTION

The release of liquid hydrocarbons into the ocean is called oil pollution. Humanity releases oil from without refining, tankers and carries out engineering actions, including piping, drilling and offshore rigs. These activities have catastrophic effects on the environment and the biology of marine life and lead to hazardous consequences. Therefore, the extent of the oil spill is essential for reciprocity. In this way, the natural ecosystem of the coastline is preserved. Also, a catastrophe is prevented in the early stages.

The area of spillage could be anticipated according to the governing equations of the fluid flow and the mass transfer phenomenon. The boundary and initial

conditions for the a calculation for diffusion of oil and change at sea can be deduced from the statistics of the the volume of oil that reaches the ocean outlet. The diffusion (parabolic) equations are the most reasonable option to model the propagation of this leakage and contamination. These equations allow statistics regarding the amount of oil that has outreached the ocean outlet, to be used as initial and boundary conditions for a mathematical model of oil diffusion and alteration in seas. Since it includes a hyperbolic section of the equation, the best options are the Allen Kahn (AC) and diffusion equations, which are challenging to solve mathematically. Several academics have investigated the production of oil and oil spill transfer based on the path method over the past three decades [1]. This method has been used for river and seas

*Corresponding Author Institutional Email: b.jalili@iau-tnb.ac.ir
(B. Jalili)

[2, 3] and lake systems [4-6]. Allen Cahn's equation is a mathematical model used to analyze the phase separation procedure in binary alloys. This equation arises in fluid dynamics as a convection-diffusion equation and materials science as a reaction-diffusion equation. When a substance changes its composition or form, phase transfer occurs at the interface. It is a straightforward model of the nonlinear reaction propagation methodology. Often employed to pinnacle interface move over time, phase separation in alloys over time is used in different fields, integrating image processing, geology, biology, bio-fluid and materials science. Sutanty et al. [7] investigated the dynamics of the modified PB DNA model by considering DNA in the Nosé-Hoover thermostat as a bio-fluid with various viscosities. In their study, viscosity variations are reviewed through temperature variations, namely thermal viscosity. They obtained the dynamical equation of DNA in the form of a nonlinear Schrödinger-like (NLS-like) equation by using the perturbation method and continuous approximation. Hariharan et al. [8] presented a Wavelet-based equivalence approach for cracking the equations for Allen-Cahn and Newell-Whitehead. The differential equation, the largest derivative was developed into the sequence of Legendre; this approximate is merged even though the boundary conditions used employing integration constants. They confirmed the conjunction of the suggested techniques. Ultimately, they have provided some numerical instances to verify the reality and relevance of the procedure. Javeed et al. [9] examine the latest exact resolutions of nonlinear fractional partial differential equations (FPDEs). The proposed technique is readily helpful and applicable, which can be executed successfully to solve various kinds of nonlinear FPDEs. Yin and Zhengyuan [10] supposed a rapid algorithm and assumed three numerical illustrations with non-smooth and smooth outcomes. They show the computational efficiency in cracking nonlinear PDEs, from which it is straightforward to see that the computing duration could be preserved. In another research, concentrating on suggesting and exploring a method for Allen-Cahn equations has been accomplished. They studied the conjunction of iterative answers. Numerical examinations were given to prove their submitted procedure.

Furthermore, it is indicated that when compared to standard finite difference iterative methods, iterative processes with extremely rare unknowns have substantially shorter computation times [11]. Khalid et al. [12] introduced a collocation technique established on redefined cubic formulation using finite differences and functions to analyze the inaccurate time-fractional Allen-Cahn equation explanation. They examined the computational efficiency of the offered approach via some numerical samples. The simulation outcomes

exhibit a definitive accord with the exact solution corresponding to those seen in the publications. In another study, Olshansky et al. [13] investigated an Allen-Cahn equation expressed on a surface that changes with time as a phase separation example with order-disorder evolution in a slim layer. A standard inner-outer expansion indicates that the solution's limiting manners are a classification flow for the geodesic mean curvature in reference coordinates. They showed a fundamental stability analysis and conjunction investigation for interpolation errors and inaccurate geometry retrieval. The diffusion equation has many applications that researchers have solved in different methods. Ahmad et al. [14] used analytical methods to solve initial value issues in ocean engineering and science. They showed the accuracy of using a technique by comparing the results to an exact solution. Patel et al. [15] approached Fractional Reduced Differential Method to solve the diffusion equation in water pollution. They proved FRDTM gives fast convergence and provides highly accurate numerical results. Lin et al. [16] simulated air pollution diffusion to analyze industrial places. They investigated industrial parks in Taiwan from 2017 to 2019. The results will aid in managing the dangers of air pollution for the petrochemical sector and public health authorities. Moraga et al. [17] studied the SIMPLER algorithm's diffusion problem in fluid flow. The results exhibit that the suggested algorithm has significant advances in reducing the number of iterations and computation time. Yan et al. [18] presented the analytical model for thermal diffusion in porous media. They assess the significance of the Soret impact and temperature dependent diffusion coefficient on non-isothermal diffusion. Hayat et al. [19] considered the thermodiffusion in unsteady magnetohydrodynamic with first order chemical reaction. They showed that compared to radiation and magnetic factors, heat transfer speed is increased. The semi-analytical approach can be utilized to solve the equations governing fluid flow [8, 20, 21] and mass transfer problems. Many researchers have used semi-analytical methods to solve various engineering problems in heat transfer [22-25] and heat pumps [26-28]. One of the essential advantages of these methods is saving time, high accuracy, and proper convergence.

The diffusion equation is a parabolic one; fluid flow depicts the visible behavior of numerous micro-particles in Brownian movement, coming about from the irregular developments and collisions of the particles (Figure 1). A diffusion process is a solution to a stochastic differential equation in probability theory and statistics. The molecule's position is at that point irregular; an advection-diffusion condition represents its likelihood thickness work as a work of space and time.

The real-world phenomenon has been governed by PDEs of integer order which cannot be adequately described. Additionally, no method gives an exact

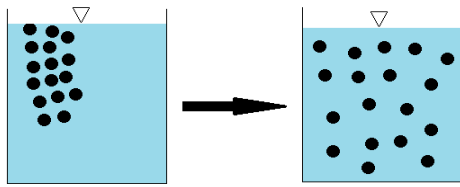


Figure 1. Scheme of diffusion trend in the water

solution for the fractional-order differential equation. Hence, nonlinear PDEs of fractional order make the research more significant. Therefore, in this paper, we have applied HPM an efficient and robust method to find the solutions to the time-fractional diffusion equation and Cahn–Allen equation arising in oil pollution. The novelty of our work is that it provides an accurate prediction of the behavior of oil and is vitally important to preserve the natural shoreline environmental system. Moreover, this method can also be applied to derive various traveling wave solutions with distinct physical structures for nonlinear fractional equations arising in ocean engineering for examining nonlinear behavior due to water waves. Equations of diffusion and Allen-Cahn were solved with different degrees of fractional derivatives ($\alpha=0.25, \alpha=0.5, \alpha=0.75$ and $\alpha=0.75$), and the oil pollution concentration was obtained at a specific time and place.

This study consists of five sections: In the first section, the topic and literature are discussed. In section two, time-Fractional diffusion is defined in both Riemann-Liouville and Caputo definitions. Also, we provide a review of the HPM and its application in section three and two presented examples illustrate the applicability and validity of the proposed method in section four. Finally, section five is the conclusion.

2. TIME-FRACTIONAL DIFFUSION

A fractional derivative of order $\alpha > 0$ is defined in many ways [29-31]. The Riemann-Liouville and Caputo definitions are the two that are the most frequently employed. Each definition makes use of whole-order derivatives and Riemann-Liouville fractional integration. In the sense of Caputo the best definitions of fractional derivatives are compiled in this section (CFD). The general diffusion equation with nonlinearity will be taken into account to describe oil contamination in the oceans, and its form is stated as follows [14]:

$$\frac{\partial \psi}{\partial t} = D \frac{\partial^2 \psi}{\partial x^2} + \beta \psi + \gamma \psi^m \tag{1}$$

where D is the diffusion coefficient, C is the concentration, β and γ are real values and ψ is concentration. An example of a diffusion equation is the Allen-Cahn (AC) equation, which is created: Substitution $\rightarrow m = 3, \gamma = -1, \beta = 1$ in Equation (1).

2. 1. Interpretation (Fractional derivative in the sense of Caputo)

If f be an integrable continual operation in (a, b) for $t \in [a, b]$ then, the left and right Caputo fractional derivatives are ${}_a^C D_t^\alpha f(t)$ and ${}_t^C D_b^\alpha f(t)$ respectively, of order α , are characterized within the following way:

$${}_a^C D_t^\alpha f(t) = \frac{1}{\Gamma(n-\alpha)} \int_a^t (t-\theta)^{n-\alpha-1} \left(\frac{d}{d\theta}\right)^n f(\theta) d\theta \tag{2}$$

$${}_t^C D_b^\alpha f(t) = \frac{1}{\Gamma(n-\alpha)} \int_t^b (\theta-t)^{n-\alpha-1} \left(-\frac{d}{d\theta}\right)^n f(\theta) d\theta \tag{3}$$

2. 2. Interpretation (Fractional derivative in the sense of Riemann-Liouville)

If f be an integrable continual operation in the interval (a, b) for $t \in [a, b]$ then, the right and left Riemann-Liouville fractional derivatives are ${}_t D_b^\alpha f(t)$ and ${}_a D_t^\alpha f(t)$ respectively of order α , are characterized by Equations (4) and (5):

$${}_a D_t^\alpha f(t) = \frac{1}{\Gamma(n-\alpha)} \left(\frac{d}{dt}\right)^n \int_a^t (t-\theta)^{n-\alpha-1} f(\theta) d\theta \tag{4}$$

$${}_t D_b^\alpha f(t) = \frac{1}{\Gamma(n-\alpha)} \left(-\frac{d}{dt}\right)^n \int_t^b (\theta-t)^{n-\alpha-1} f(\theta) d\theta \tag{5}$$

where $n \in N, n - 1 \leq \alpha < n$ and Γ is the Euler Gamma Function.

In both definitions, if $\alpha \in N$, give the classical derivatives, and the A constant's Caputo fractional derivative is always equal to zero.

3. HOMOTOPY PERTURBATION METHOD

We will provide a review of the HPM in this part. Numerous records provide information on the HPM's concepts and their applicability to numerous types of differential equations [22, 24, 32]. Consider the nonlinear differential equation.

We look at the following equation to demonstrate the fundamental concepts behind this approach:

$$X(u) - z(r) = 0. \quad r \in \Omega \tag{6}$$

Having a boundary condition:

$$Y\left(u, \frac{\partial u}{\partial n}\right) = 0. \quad r \in \Gamma \tag{7}$$

$z(r)$ is a well-known analytical function, X is a generic differential operator, Y is a boundary operator and Γ is the domain boundary of Ω and L is linear and N is nonlinear, can be used to split the variable X . Therefore, Equation (10) may be expressed as follows:

$$N(u) + L(u) - z(r) = 0. \quad r \in \Omega \tag{8}$$

The following is a diagram of the homotopy perturbation structure:

$$H(v, p) = (1-p)[L(v) - L(u_0)] + p[X(v) - z(r)] = 0. \tag{9}$$

And:

$$v(r, p) : \Omega \times [0, 1] \rightarrow R \tag{10}$$

$p \in [0, 1]$ is a parameter of embedding and u_0 is the initial approximation that meets the boundary requirement. Equation (11)'s answer can be expressed as a power series in p , as shown below:

$$v = v_0 + pv_1 + p^2v_2 + \dots \tag{11}$$

The following approximates the answer to the question:

$$u = \lim_{p \rightarrow 1} v = v_0 + v_1 + v_2 + \dots \tag{12}$$

3. 1. Application of HPM To obtain the behavior of the Allen-Cahn condition and the dissemination condition.

- Time-fractional diffusion equation

$$\frac{\partial^\alpha \psi}{\partial t^\alpha} = \frac{\partial^2 \psi}{\partial x^2} + \cos x \tag{13}$$

- The Allen-Cahn equation with time fractions

$$\frac{\partial^\alpha \psi}{\partial t^\alpha} = \frac{\partial^2 \psi}{\partial x^2} + \psi - \psi^3 \tag{14}$$

In this paper, the research methodology flowchart is shown in Figure 2. Problem identification is actually seeing the problem before trying to solve it. In other word, it is a first strategy in solving a problem. Numerical solution involves solving the equation by the HPM method, which, if solved, the answer will be validated by the exact solution following literature [14]. This process is repeated until an accurate answer is reached.

4. INFORMATIVE EXAMPLES

To demonstrate the effectiveness of the Homotopy Perturbation Method (HPM), we consider the following Fractional Differential Equations (FDEs) in sense of Caputo type. All the results were calculated by using the symbolic calculus Maple software. Further, the results of the hybrid approach are implemented in Maple software.

Example 4.1

Consider the time-fractional AC Equation (15) and having the initial condition as follows [14]:

$$\frac{\partial^\alpha \psi}{\partial t^\alpha} = \frac{\partial^2 \psi}{\partial x^2} + \psi - \psi^3, \quad 0 < \alpha \leq 1 \tag{15}$$

$$\psi(x, 0) = \frac{1}{2} \tanh(0.3536x) - \frac{1}{2}, \tag{16}$$

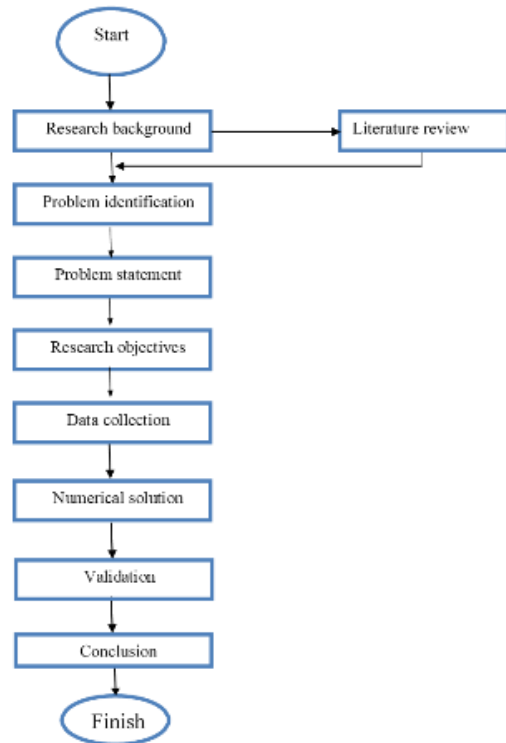


Figure 2. The research methodology flowchart

For $\alpha = 1$, the exact answer to Equation (15) is [14].

$$\psi(x, 0) = \frac{1}{2} \tanh(0.3536x - 0.75t) - \frac{1}{2} \tag{17}$$

4. 1. 1. Application of HPM For applying the HPM on Equation (15), according to Equation (16) as an initial condition, we have

$$equ := \int_0^t \frac{0.5641895835(\frac{\partial}{\partial t} \psi(x, \tau))}{(t-\tau)^{0.5}} d\tau - \left(\frac{\partial^2}{\partial x^2} \psi(x, \tau) \right) - \psi(x, \tau) + \psi(x, \tau)^3 = 0 \tag{18}$$

For applying the HPM on Equation (15), the homotopy form of the fractional differential equation should be written. Next, we take into account an approximate solution to the issue in terms of the different powers of P in series. Equation (26), which successfully merges to the precise answer $\psi(x, 0) = \frac{1}{2} \tanh(0.3536x - 0.75t) - \frac{1}{2}$, provides the analytical approximation of the fractional order in time of Equation (15).

The effects of "t" on the solution of the AC equation are depicted in Figures 3 and 4 in accordance with the I.C $\psi(x, 0) = \frac{1}{2} + \frac{1}{2} \tanh(0.3536x)$. Figure 5 also includes the three-dimensional charts. Figures 3 and 4 show the curved nonlinearity is seen for lower amounts of α , but that there are less nonlinear developments when is closer to 1 ($\alpha = 0.25, 0.5, 0.75$). The outcomes have been

contrasted with the precise answer that is currently known for integer-order $\alpha = 1$. Figures 3 and 4 display the variations ψ for various values of α . Figure 3 also displays the outcomes for $t=0.5$, and Figure 4 displays the outcomes for $t=1$. Figure 5 is three-dimensional plot for the changes of $\psi(x,t)$ and Figure 6 is Abs. Error graph by HPM and MVIA-I [14] for example 1.

$$\psi(x, t) = \psi_0(x, t) + P\psi_1(x, t) + P^2\psi_2(x, t) + P^3\psi_3(x, t) + P^4\psi_4(x, t) \tag{19}$$

$$\begin{aligned} & \frac{\partial}{\partial t} \psi_0(x, t) + P \left(\frac{\partial}{\partial t} \psi_1(x, t) \right) + P^2 \left(\frac{\partial}{\partial t} \psi_2(x, t) \right) + \\ & P^3 \left(\frac{\partial}{\partial t} \psi_3(x, t) \right) + P^4 \left(\frac{\partial}{\partial t} \psi_4(x, t) \right) = \\ & P \left(\frac{\partial}{\partial t} \psi_0(x, t) + P \left(\frac{\partial}{\partial t} \psi_1(x, t) \right) + \right. \\ & P^2 \left(\frac{\partial}{\partial t} \psi_2(x, t) \right) + P^3 \left(\frac{\partial}{\partial t} \psi_3(x, t) \right) + \\ & P^4 \left. \left(\frac{\partial}{\partial t} \psi_4(x, t) \right) \right) - \\ & \left(\int_0^t \frac{0.5641895835 \left(\frac{\partial}{\partial \tau} \psi_0(x, t) + P + P^2 + P^3 + P^4 \right)}{(t-\tau)^{0.5}} d\tau \right) + \\ & \left(\frac{\partial^2}{\partial x^2} \psi_0(x, t) + P \left(\frac{\partial^2}{\partial x^2} \psi_1(x, t) \right) + \right. \\ & P^2 \left(\frac{\partial^2}{\partial x^2} \psi_2(x, t) \right) + P^3 \left(\frac{\partial^2}{\partial x^2} \psi_3(x, t) \right) + \\ & P^4 \left. \left(\frac{\partial^2}{\partial x^2} \psi_4(x, t) \right) \right) + P\psi_1(x, t) + P^2\psi_2(x, t) + \\ & P^3\psi_3(x, t) + P^4\psi_4(x, t) - (\psi_0(x, t) + P\psi_1(x, t) + \\ & P^2\psi_2(x, t) + P^3\psi_3(x, t) + P^4\psi_4(x, t)^3) \end{aligned} \tag{20}$$

Then, we should define BCs

$$\psi(x, 0) = \frac{1}{2} \tanh(0.3536x) - \frac{1}{2}, \tag{21}$$

After substituting initial conditions into Equation (20) and we putting $P=I$ in each equation we have

$$\psi_0(x, t) = -\frac{1}{2} + \frac{1}{2} \tanh\left(\frac{221}{625}x\right) \tag{22}$$

$$\psi_1(x, t) = \frac{1}{3125000} \frac{t(103 \sinh(\frac{221}{625}x)) + t(1171875 \cosh(\frac{221}{625}x))}{\cosh(\frac{221}{625}x)^3} \tag{23}$$

$$\begin{aligned} \psi_2(x, t) = & -\frac{309}{6250000} \frac{1}{\cosh(\frac{221}{625}x)^5} \left(t \left(\left(\frac{781250}{103} + \right. \right. \right. \\ & t) \cosh\left(\frac{221}{625}x\right)^3 + \left. \left. \left(\frac{2}{3} + \right. \right. \right. \\ & \left. \left. \frac{686645513117}{120703125} t \right) \sinh\left(\frac{221}{625}x\right) \cosh\left(\frac{221}{625}x\right)^2 - \right. \\ & \left. \left. \left. \frac{5}{4} \cosh\left(\frac{221}{625}x\right) t - \frac{390831}{1562500} t \sinh\left(\frac{221}{625}x\right) \right) \right) \right) \end{aligned} \tag{24}$$

$$\begin{aligned} \psi_3(x, t) = & \frac{1}{45776367187500000000} \cdot \\ & \frac{1}{\cosh(\frac{221}{625}x)^7} \left((-6437301784931250000 t^3 - \right. \\ & \left. 4526367187500000 t^2 - \right. \end{aligned} \tag{25}$$

$$\begin{aligned} & 17166137695312500000 t) \cosh\left(\frac{221}{625}x\right)^5 + \\ & (-1697387699683408 t^3 - \\ & 25749206741887500000 t^2 - \\ & 1508789062500000 t) \sinh\left(\frac{221}{625}x\right) \cosh\left(\frac{221}{625}x\right)^4 + \\ & 9657084915679687500 t^2 \left(t + \right. \\ & \left. \frac{241406250}{412035623069} \cosh\left(\frac{221}{625}x\right)^3 + \right. \\ & \left. 3960820003063620 \left(t + \right. \right. \\ & \left. \left. \frac{183202031250}{640909385609} \sinh\left(\frac{221}{625}x\right) t^2 \cosh\left(\frac{221}{625}x\right)^2 - \right. \right. \\ & \left. \left. 368135762890625 \cosh\left(\frac{221}{625}x\right) t^3 - \right. \right. \\ & \left. \left. 566255996392305 \sinh\left(\frac{221}{625}x\right) t^3 \right) \right) \end{aligned}$$

After simplifying and solving the problem, we have

$$\begin{aligned} \psi_3(x, t) = & -\frac{1}{2} + \frac{1}{2} \tanh\left(\frac{221}{625}x\right) - \\ & \frac{1}{3125000} \frac{t(103 \sinh(\frac{221}{625}x) + 1171875 \cosh(\frac{221}{625}x))}{\cosh(\frac{221}{625}x)^3} - \\ & \frac{309}{6250000} \frac{1}{\cosh(\frac{221}{625}x)^5} \left(t \left(\left(\frac{781250}{103} + t \right) \cosh\left(\frac{221}{625}x\right)^3 + \right. \right. \\ & \left. \left. \left(\frac{2}{3} + \frac{686645513117}{120703125} t \right) \sinh\left(\frac{221}{625}x\right) \cosh\left(\frac{221}{625}x\right)^2 - \right. \right. \\ & \left. \left. \frac{5}{4} \cosh\left(\frac{221}{625}x\right) t - \frac{390831}{1562500} t \sinh\left(\frac{221}{625}x\right) \right) \right) \end{aligned} \tag{26}$$

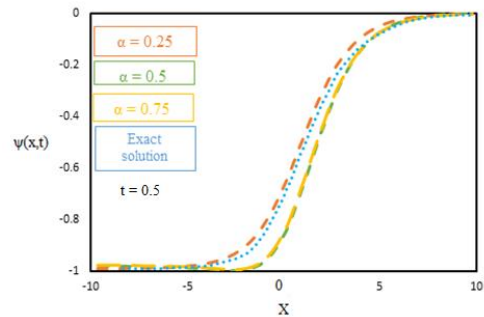


Figure 3. The changes of $\psi(x,t)$ to X in different values of α in $t=0.5$

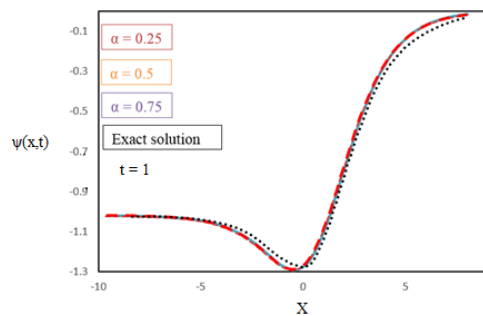


Figure 4. The changes of $\psi(x,t)$ to X in different values of α in $t=1$

TABLE 1. Comparison of absolute errors for different values for Example 1

x	t=1				t=0.5			
	HPM	MVIA-I [14]	LLWM [8]	ADM [24]	HPM	MVIA-I [7]	LLWM [8]	ADM [24]
-25	1.16529E-10	1.17373E-10	1.18943E-11	1.1644E-11	1.24869E-10	1.25342E-10	6.4747E-12	1.45683E-6
-15	1.37844E-07	1.38319E-07	2.36636E-9	1.37206E-8	1.47136E-07	1.47721E-07	1.35653E-10	1.23638E-9
25	1.58218E-10	1.57665E-10	9.84744E-10	4.8392E-10	1.69113E-09	1.68402E-09	7.49924E-10	1.35958E-8
30	4.60177 E-12	4.59300 E-12	3.57575E-11	1.4096E-11	4.90841E-12	4.90550E-12	2.44443E-10	3.9604E-10

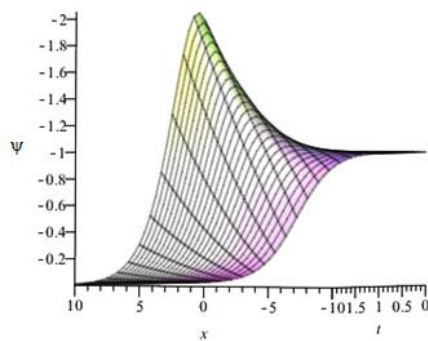


Figure 5. Three-dimensional plot for the changes of $\psi(x,t)$

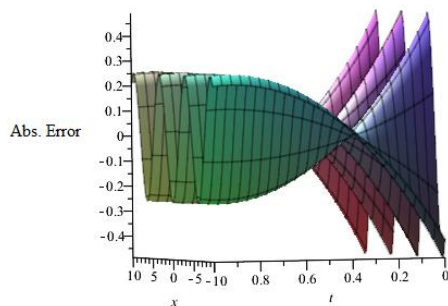


Figure 6. Abs. error graph by HPM and MVIA-I [14]

Example 4.2

Consider the diffusion Equation (27) and having the initial condition as follows [14]:

$$\frac{\partial^\alpha \psi}{\partial t^\alpha} = \frac{\partial^2 \psi}{\partial x^2} + \cos x, \quad 0 < \alpha \leq 1 \tag{27}$$

$$\psi(x, 0) = 0 \tag{28}$$

For $\alpha = 1$, there is an accurate solution to Equation (27) [7]:

$$\psi(x, t) = \cos x (1 - e^{-t}) \tag{29}$$

4. 2. 1. Application of HPM

For applying the homotopy perturbation method on Equation (27),

according to the Equation (28) as an initial condition, we have:

$$\begin{aligned} equ := & \int_0^t \frac{0.5641895835 \left(\frac{\partial}{\partial t} \psi(x, \tau) \right)}{(t-\tau)^{0.5}} d\tau - \\ & \left(\frac{\partial^2}{\partial x^2} \psi(x, \tau) \right) - \cos(x) = 0 \end{aligned} \tag{30}$$

For applying the HPM on Equation (15), the homotopy form of the FDE should be written. The problem's approximation is then considered in terms of the various powers of P in series.

$$\psi(x, t) = \psi_0(x, t) + P\psi_1(x, t) + P^2\psi_2(x, t) + P^3\psi_3(x, t) \tag{31}$$

$$\begin{aligned} & \frac{\partial}{\partial t} \psi_0(x, t) + P \left(\frac{\partial}{\partial t} \psi_1(x, t) \right) + P^2 \left(\frac{\partial}{\partial t} \psi_2(x, t) \right) + \\ & P^3 \left(\frac{\partial}{\partial t} \psi_3(x, t) \right) = P \left(\frac{\partial}{\partial t} \psi_0(x, t) + \right. \\ & P \left(\frac{\partial}{\partial t} \psi_1(x, t) \right) + P^2 \left(\frac{\partial}{\partial t} \psi_2(x, t) \right) + \\ & P^3 \left(\frac{\partial}{\partial t} \psi_3(x, t) \right) \left. \right) - \\ & \left(\int_0^t \frac{0.5641895835 \left(\frac{\partial}{\partial t} \psi_0(x, t) + P + P^2 + P^3 \right)}{(t-\tau)^{0.5}} d\tau \right) + \\ & \left(\frac{\partial^2}{\partial x^2} \psi_0(x, t) + P \left(\frac{\partial^2}{\partial x^2} \psi_1(x, t) \right) + \right. \\ & P^2 \left(\frac{\partial^2}{\partial x^2} \psi_2(x, t) \right) + P^3 \left(\frac{\partial^2}{\partial x^2} \psi_3(x, t) \right) \left. \right) + \\ & \cos(x) \end{aligned} \tag{32}$$

Then, we should define boundary conditions

$$\psi_i(x, t) = 0, \quad i = 0, \dots, 3 \tag{33}$$

After substituting initial conditions into Equation (32) and we putting $P=I$ in each equation we have:

$$\psi_0(x, t) = 0 \tag{34}$$

$$\psi_1(x, t) = \cos(x) t \tag{35}$$

$$\psi_2(x, t) = -\frac{1}{2} \cos(x) t \left(t + \frac{376126389}{250000000} \sqrt{t} - 2 \right) \tag{36}$$

and simplifying and solving the problem, we have

$$\psi(x, t) = \cos(x) t - \frac{1}{2} \cos(x) t \left(t + \frac{376126389}{250000000} \sqrt{t-2} \right) \tag{37}$$

The time-fractional diffusion problem's approximate analytical solution is shown in Equation (37) and the series solution efficiently converges for precise solution $\psi(x, t) = \cos x (1 - e^{-t})$ as $\alpha \rightarrow 1$. Figures 7 and 8 illustrate the effects of 't' (t=0.5 and t=1) on the solution of the AC equation in accordance by the initial condition $\psi(x, 0) = 0$. Figure 9 also include the three-dimensional graphs. Figures 7 and 8 show that the curved nonlinearity is seen for lower values of, but that less nonlinear developments are seen as approaches 1 ($\alpha = 0.25, 0.5, \text{ and } 0.75$). The outcomes have been contrasted with the precise answer that is currently known for integer-order = 1. Figure 9 shows three-dimensional plot for the changes of $\psi(x, t)$, and Figure 10 is Abs. Error graph by HPM and MVIA-I [14] for example 2.

Comparison of absolute errors of HPM, MVIA-I [14], and VIA-I [15] for different values of parameters x and t is given in Tables 1 and 2, show that the error in HPM is less as compared to MVIT-I and VIA-I. Moreover, we considered only five iterations which are less than those in MVIT-I [14] and VIA-I [15]. This saves computational time and give better result. The numerical results for AC equations are reported in Tables 1 and 2. To prove the effectiveness of the planned techniques, absolute errors

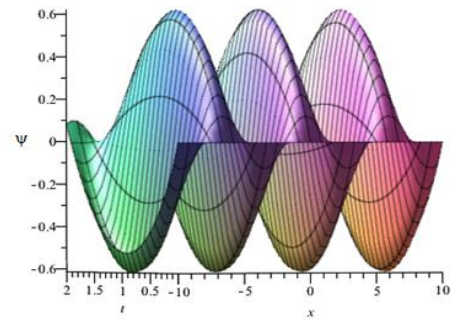


Figure 9. 3D plot for the variation of $\psi(x, t)$

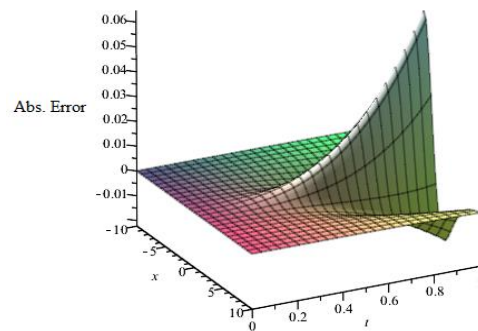


Figure 10. Abs. error graph by HPM and MVIA-I [14] for example 2

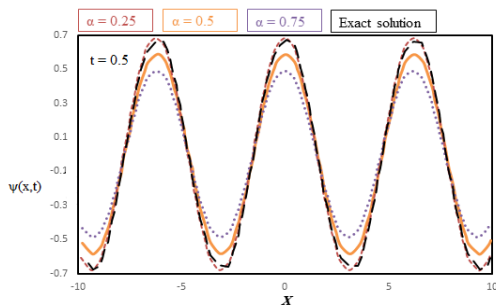


Figure 7. The changes of $\psi(x, t)$ to X in different values of α in $t=0.5$

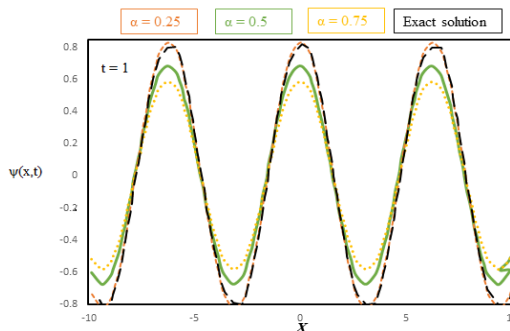


Figure 8. The changes of $\psi(x, t)$ to X in different values of α in $t=1$

TABLE 2. Comparison of numerical results for different values of x and t for Example 2

x	t	Abs. error in HPM	Abs. error in MVIA – I [14]	Abs. error in VIA – I [15]
1	0.5	1.242E-10	1.671E-10	6.344E-10
2	1.0	0.000E+00	3.563E-10	9.619E-09
3	1.5	2.398E-10	2.683E-09	1.905E-06
4	2.0	0.000E+00	1.871E-08	2.870E+05
5	2.5	3.667E-10	5.510E-08	1.399E-04
6	3.0	0.000E+00	5.522E-07	3.398E-03
7	3.5	2.8430E-10	2.929E-06	1.406E-02
8	4.0	0.000E+00	8.666E-07	1.141E-02
9	4.5	5.160E-09	8.689E-06	2.528E-01
10	5.0	2.600E-09	1.682E-05	7.193E-01

are reported along with the results of other methods; MVIA – I [14], ADM [47], VIA – I [15] and LLWM [1]. In comparison with other techniques results, one can ensure that the results of HPM are more precise. It is cleared from figures that the proposed method can handle the problems accurately and will be applicable in ocean engineering for studying linear and nonlinear water waves.

5. CONCLUSION

Oil pollution is defined as the emission of fluid hydrocarbon into the ocean which causes disastrous effects on marine life's eco and biological environment and leads to fatal repercussions. Thus, it is crucial to precisely predict the spread range of oil spills for an early stage countermeasure against a disaster to preserve the natural shoreline environmental system. For these reasons, in this study, the homotopy perturbation approach is used to generate approximations for the diffusion equation occurring in oil pollution in water for three different fractional orders, $\alpha = 0.25$, $\alpha = 0.5$, and $\alpha = 0.75$; and integer-order, $\alpha = 1.0$; Also, several types of AC equations are obtained using the homotopy perturbation method (HPM). Additionally, it may be used in diffusion equations for both linear and non-linear analyses of marine oil contamination. The results show that the HPM can tackle the problems perfectly, and it can be deployed in diffusion equations for analyzing oil pollution in the sea with linear and non-linear nature. The absolute error diagrams show good accuracy of the applied technique compare to MVIA-I [14] and prove that this method can be used in many scientific and engineering problems and provides highly accurate numerical results without using Adomian polynomials, discretization, transformation, shape parameters, restrictive assumptions, or linearization for nonlinear time-fractional differential equations. As with every other study, our study has had certain limitations. This study focused on the homotopy perturbation method (HPM) and was validated with the MVIA-I method. So for future work, it is highly recommended to solve diffusion equations by VIM and AGM methods.

6. REFERENCES

- Spaulding, M.L., "A state-of-the-art review of oil spill trajectory and fate modeling", *Oil and Chemical Pollution*, Vol. 4, No. 1, (1988), 39-55. [https://doi.org/10.1016/S0269-8579\(88\)80009-1](https://doi.org/10.1016/S0269-8579(88)80009-1)
- Shen, H.T. and Yapa, P.D., "Oil slick transport in rivers", *Journal of Hydraulic Engineering*, Vol. 114, No. 5, (1988), 529-543. [https://doi.org/10.1061/\(ASCE\)0733-9429\(1988\)114:5\(529\)](https://doi.org/10.1061/(ASCE)0733-9429(1988)114:5(529))
- Yapa, P.D., Shen, H.T. and Angamma, K.S., "Modeling oil spills in a river—lake system", *Journal of Marine Systems*, Vol. 4, No. 6, (1994), 453-471. [https://doi.org/10.1016/0924-7963\(94\)90021-3](https://doi.org/10.1016/0924-7963(94)90021-3)
- Lonin, S.A., "Lagrangian model for oil spill diffusion at sea", *Spill Science & Technology Bulletin*, Vol. 5, No. 5-6, (1999), 331-336. [https://doi.org/10.1016/S1353-2561\(99\)00078-X](https://doi.org/10.1016/S1353-2561(99)00078-X)
- Wang, S., Shen, Y. and Zheng, Y., "Two-dimensional numerical simulation for transport and fate of oil spills in seas", *Ocean Engineering*, Vol. 32, No. 13, (2005), 1556-1571. <https://doi.org/10.1016/j.oceaneng.2004.12.010>
- Wang, S.-D., Shen, Y.-M., Guo, Y.-K. and Tang, J., "Three-dimensional numerical simulation for transport of oil spills in seas", *Ocean Engineering*, Vol. 35, No. 5-6, (2008), 503-510. <https://doi.org/10.1016/j.oceaneng.2007.12.001>
- Sutantyo, T., Ripai, A., Abdullah, Z., Hidayat, W. and Zen, F.P., "Soliton-like solution on the dynamics of modified peyrard-bishop DNA model in the thermostat as a bio-fluid", *Emerg. Sci. J. (ISSN: 2610-9182)*, Vol. 6, No. 4, (2022). doi: 10.28991/ESJ-2022-06-04-01.
- Hariharan, G., "An efficient legendre wavelet-based approximation method for a few newell–whitehead and allen–cahn equations", *The Journal of Membrane Biology*, Vol. 247, No. 5, (2014), 371-380. <https://doi.org/10.1007/s00232-014-9638-z>
- Javeed, S., Saif, S. and Baleanu, D., "New exact solutions of fractional cahn–allen equation and fractional dsw system", *Advances in Difference Equations*, Vol. 2018, No. 1, (2018), 1-15. <https://doi.org/10.1186/s13662-018-1913-3>
- Yin, B., Liu, Y., Li, H. and He, S., "Fast algorithm based on tt-m fe system for space fractional allen–cahn equations with smooth and non-smooth solutions", *Journal of Computational Physics*, Vol. 379, (2019), 351-372. <https://doi.org/10.1016/j.jcp.2018.12.004>
- Li, H. and Song, Z., "A reduced-order energy-stability-preserving finite difference iterative scheme based on pod for the allen–cahn equation", *Journal of Mathematical Analysis and Applications*, Vol. 491, No. 1, (2020), 124245. <https://doi.org/10.1016/j.jmaa.2020.124245>
- Khalid, N., Abbas, M., Iqbal, M.K. and Baleanu, D., "A numerical investigation of caputo time fractional allen–cahn equation using redefined cubic b-spline functions", *Advances in Difference Equations*, Vol. 2020, No. 1, (2020), 1-22. <https://doi.org/10.1186/s13662-020-02616-x>
- Olshanskii, M., Xu, X. and Yushutin, V., "A finite element method for allen–cahn equation on deforming surface", *Computers & Mathematics with Applications*, Vol. 90, (2021), 148-158. <https://doi.org/10.1016/j.camwa.2021.03.018>
- Ahmad, H., Khan, T.A., Durur, H., Ismail, G. and Yokus, A., "Analytic approximate solutions of diffusion equations arising in oil pollution", *Journal of Ocean Engineering and Science*, Vol. 6, No. 1, (2021), 62-69. <https://doi.org/10.1016/j.joes.2020.05.002>
- Patel, H., Patel, T. and Pandit, D., "An efficient technique for solving fractional-order diffusion equations arising in oil pollution", *Journal of Ocean Engineering and Science*, (2022). <https://doi.org/10.1016/j.joes.2022.01.004>
- Lin, Y.-C., Lai, C.-Y. and Chu, C.-P., "Air pollution diffusion simulation and seasonal spatial risk analysis for industrial areas", *Environmental Research*, Vol. 194, (2021), 110693. <https://doi.org/10.1016/j.envres.2020.110693>
- Moraga, N.O., Jaime, J.I. and Cabrales, R.C., "An approach to accelerate the convergence of simpler algorithm for convection-diffusion problems of fluid flow with heat transfer and phase change", *International Communications in Heat and Mass Transfer*, Vol. 129, (2021), 105715. <https://doi.org/10.1016/j.icheatmasstransfer.2021.105715>
- Yan, H., Sedighi, M. and Xie, H., "Thermally induced diffusion of chemicals under steady-state heat transfer in saturated porous media", *International Journal of Heat and Mass Transfer*, Vol. 153, No., (2020), 119664. <https://doi.org/10.1016/j.ijheatmasstransfer.2020.119664>
- Hayat, T., Khan, S.A. and Momani, S., "Finite difference analysis for entropy optimized flow of casson fluid with thermo diffusion and diffusion-thermo effects", *International Journal of Hydrogen Energy*, Vol. 47, No. 12, (2022), 8048-8059. <https://doi.org/10.1016/j.ijhydene.2021.12.093>
- Domiri-Ganji, D., Jalili, B., Jalili, P., Shateri, A. and Mousavi, A., "Thermal analysis of fluid flow with heat generation for different logarithmic surfaces", *International Journal of Engineering*,

- Transactions C: Aspects*, Vol. 35, No. 12, (2022). doi: 10.5829/IJE.2022.35.12C.03.
21. Jalili, B., Sadighi, S., Jalili, P. and Ganji, D.D., "Characteristics of ferrofluid flow over a stretching sheet with suction and injection", *Case Studies in Thermal Engineering*, Vol. 14, No., (2019), 100470. <https://doi.org/10.1016/j.csite.2019.100470>
 22. Jalili, P., Ganji, D.D., Jalili, B. and Ganji, D.R.M., "Evaluation of electro-osmotic flow in a nanochannel via semi-analytical method", *Thermal Science*, Vol. 16, No. 5, (2012), 1297-1302. doi: 10.2298/TSCI1205297J.
 23. Jalili, P., Ganji, D. and Nourazar, S., "Hybrid semi analytical method for geothermal u shaped heat exchanger", *Case Studies in Thermal Engineering*, Vol. 12, No., (2018), 578-586. <https://doi.org/10.1016/j.csite.2018.07.010>
 24. Gui, C. and Zhao, M., "Traveling wave solutions of allen-cahn equation with a fractional laplacian", in *Annales de l'Institut Henri Poincaré C, Analyse non linéaire*, Elsevier. Vol. 32, (2015), 785-812.
 25. Pasha, P., Nabi, H., Peiravi, M.M. and Ganji, D.D., "Hybrid investigation of thermal conductivity and viscosity changeable with generation/absorption heat source", *Computational Thermal Sciences: An International Journal*, Vol. 14, No. 1, (2022). doi. 10.1615/ComputThermalScien.2021039390
 26. Farid, Z., Lamdouar, N. and Ben Bouziyane, J., "A method of strip footings design for light structures on expansive clays", *International Journal of Engineering, Transactions A: Basics* Vol. 35, No. 1, (2022), 248-257. doi: 10.5829/IJE.2022.35.01A.24.
 27. Jalili, B., Aghaee, N., Jalili, P. and Ganji, D.D., "Novel usage of the curved rectangular fin on the heat transfer of a double-pipe heat exchanger with a nanofluid", *Case Studies in Thermal Engineering*, (2022), 102086. <https://doi.org/10.1016/j.csite.2022.102086>
 28. Tarrad, A.H., "3d numerical modeling to evaluate the thermal performance of single and double u-tube ground-coupled heat pump", *HighTech and Innovation Journal*, Vol. 3, No. 2, (2022), 115-129. doi: 10.28991/HIJ-2022-03-02-01.
 29. Cresson, J., "Fractional embedding of differential operators and lagrangian systems", *Journal of Mathematical Physics*, Vol. 48, No. 3, (2007), 033504. <https://doi.org/10.1063/1.2483292>
 30. Kilbas, A.A., Srivastava, H.M. and Trujillo, J.J., "Theory and applications of fractional differential equations, elsevier, Vol. 204, (2006).
 31. Miller, K.S. and Ross, B., "An introduction to the fractional calculus and fractional differential equations, Wiley, (1993).
 32. Jalili, B., Jalili, P., Sadighi, S. and Ganji, D.D., "Effect of magnetic and boundary parameters on flow characteristics analysis of micropolar ferrofluid through the shrinking sheet with effective thermal conductivity", *Chinese Journal of Physies*, Vol. 71, (2021), 136-150. <https://doi.org/10.1016/j.cjph.2020.02.034>

Persian Abstract

چکیده

نشت نفت در دریاها و اقیانوس ها باعث آلودگی می شود و اثرات مخرب زیست محیطی زیادی دارد. معادلات انتشار (پارابولیک) معقول ترین گزینه برای مدل سازی انتشار این نشت و آلودگی است. این معادلات اجازه می دهد تا آمار مربوط به مقدار نفتی که به خروجی اقیانوس رسیده است، به عنوان شرایط اولیه و مرزی برای مدل ریاضی انتشار و تغییر نفت در دریاها مورد استفاده قرار گیرد. از آنجایی که شامل مولفه هذلولی (فرار/موج) معادله می شود، معقول ترین انتخاب معادلات انتشار و آلن کان (AC) است که حل عددی آنها دشوار است. معادلات انتشار و آلن کان با درجات مختلفی از مشتقات کسری حل شد $\alpha = 0/25, \alpha = 0/5, \alpha = 0/75$ و $\alpha = 0/75$ و غلظت آلودگی نفتی در زمان و مکان مشخصی به دست آمد. روش اغتشاش هموتویی (HPM) برای معادله غیرخطی آلن-کان (AC) و معادله انتشار کسری زمان برای بیان آلودگی نفتی در آب. دو مثال ارائه شده کاربرد و اعتبار روش پیشنهادی را نشان می دهد. غلظت آلودگی در میدان جریان در یک بازه زمانی و مکانی برای درجات مختلف اشتقاق کسری نشان داده شده است. در درجات مشتق کسر کمتر، رفتار غلظت آلودگی غیرخطی است و با افزایش درجه مشتق کسر به یک، رفتار غیرخطی غلظت آلودگی کاهش می یابد. نتایج حاصل از تکنیک پیشنهادی در مقایسه با راه حل های دقیق نشان می دهد که این روش کارآمد و راحت بوده و زمان محاسباتی را کاهش می دهد.
